THE JOURNAL OF BIOLOGICAL CHEMISTRY
Vol. 279, No. 6, Issue of February 6, pp. 4376–4385, 2004

Printed in U.S.A.

Mechanism of Loading the *Escherichia coli* DNA Polymerase III Sliding Clamp

I. TWO DISTINCT ACTIVITIES FOR INDIVIDUAL ATP SITES IN THE γ COMPLEX*

Received for publication, September 22, 2003, and in revised form, November 3, 2003
Published, JBC Papers in Press, November 10, 2003, DOI 10.1074/jbc.M310429200

Christopher R. Williams‡, Anita K. Snyder‡, Petr Kuzmič§, Mike O'Donnell¶, and Linda B. Bloom‡‖

From the ‡Department of Biochemistry and Molecular Biology, University of Florida, Gainesville, Florida 32610-0245, §Biokin, Limited, Pullman, Washington 99163, and the ¶Rockefeller University and Howard Hughes Medical Institute, New York, New York 10021

The *Escherichia coli* DNA polymerase III γ complex loads the β clamp onto DNA, and the clamp tethers the core polymerase to DNA to increase the processivity of synthesis. ATP binding and hydrolysis promote conformational changes within the γ complex that modulate its affinity for the clamp and DNA, allowing it to accomplish the mechanical task of assembling clamps on DNA. This is the first of two reports (Snyder, A. K., Williams, C. R., Johnson, A., O'Donnell, M., and Bloom, L. B. (2004) *J. Biol. Chem.* 279, 4386–4393) addressing the question of how ATP binding and hydrolysis modulate specific interactions with DNA and β. Pre-steady-state rates of ATP hydrolysis were slower when reactions were initiated by addition of ATP than when the γ complex was equilibrated with ATP and were limited by the rate of an intramolecular reaction, possibly ATP-induced conformational changes. Kinetic modeling of assays in which the γ complex was incubated with ATP for different periods of time prior to adding DNA to trigger hydrolysis suggests a mechanism in which a relatively slow conformational change step ($k_{forward} = 6.5\ s^{-1}$) produces a species of the γ complex that is activated for DNA (and β) binding. In the absence of β, 2 of the 3 molecules of ATP are hydrolyzed rapidly prior to releasing DNA, and the 3rd molecule is hydrolyzed slowly. In the presence of β, all 3 molecules of ATP are hydrolyzed rapidly. These results suggest that hydrolysis of 2 molecules of ATP may be coupled to conformational changes that reduce interactions with DNA, whereas hydrolysis of the 3rd is coupled to changes that result in release of β.

Sliding clamps increase the overall efficiency of DNA synthesis by tethering DNA polymerases to the templates. In the absence of the sliding clamp, *Escherichia coli* DNA polymerase III is capable of incorporating about one dozen nucleotides in a single binding event. However, when it is bound to the β sliding clamp, the processivity of the DNA polymerase III core (composed of the α, ε, and θ subunits) increases to thousands of nucleotides (1). Sliding clamps remain tightly associated with template DNA while, at the same time, allowing the polymerase to move rapidly along DNA as it incorporates nucleotides. This is possible because the clamps are composed of protein subunits that are assembled in a ring-shaped structure with a central opening large enough to encircle duplex DNA (2). The *E. coli* β clamp is composed of two identical crescent-shaped monomers, whereas the human proliferating cell nuclear antigen clamp contains three, but the overall structures of both complexes are strikingly similar (2, 3).

The activity of a clamp loader is required to assemble these ring-shaped sliding clamps around DNA. The *E. coli* DNA polymerase III clamp loader is composed of seven different subunits; three copies of the *dnaX* gene product; and a single copy each of δ, δ′, χ, and ψ (4–6). The *dnaX* gene produces two proteins: a full-length protein (τ) and a truncated protein (γ). The γ subunit is about two-thirds the length of τ and is created by a translational frameshift (7–9). The additional C-terminal 24 kDa present on τ allows τ to coordinate the activities of the replisome. The τ subunit binds the core polymerase, tethering the clamp loader to the polymerase (10–14); interacts with the DnaB helicase to couple DNA synthesis to fork progression (15–17); and promotes dissociation of the polymerase from a completed Okazaki fragment, facilitating recycling of the lagging strand polymerase to the next primer to be extended (18, 19). The activities of the DnaX proteins that are required for clamp loading are contained in both the τ and γ subunits; and clamp loaders containing either τ or γ, referred to as the τ complex ($\tau_3\delta\delta'\chi\psi$) or the γ complex ($\gamma_3\delta\delta'\chi\psi$), respectively, are fully active (5, 18, 20).

The mechanical task of assembling clamps on DNA requires that protein-protein and protein-DNA interactions change during a single cycle of a clamp loading reaction. The clamp loader must initially have a high affinity for clamps and DNA to bring the clamp to DNA, but then must have a decreased affinity to release the clamp on DNA and to avoid competing with the polymerase for loaded clamps. ATP binding and hydrolysis by the DnaX subunits drive conformational changes within the clamp loader that rapidly modulate its affinity for clamps and DNA. This change in affinity must be rapid enough to support DNA synthesis on the lagging strand, where a clamp must be loaded for every 1–2-kb Okazaki fragment that is synthesized every 1–2 s.

Modulation of the β and DNA binding activities of the clamp loader requires the coordinated activities of a minimum of five of the seven γ complex subunits, three γ subunits, δ, and δ′ (21–24). The δ subunit of the *E. coli* clamp loader alone is capable of binding the β clamp and opening a dimer interface (25–28). These interactions are inhibited by the δ′ subunit,

* This work was supported by National Institutes of Health Grants GM55596 (to L. B. B.) and GM38839 (to M. O.) and by National Science Foundation Training Grant DBI-9602258. The costs of publication of this article were defrayed in part by the payment of page charges. This article must therefore be hereby marked "*advertisement*" in accordance with 18 U.S.C. Section 1734 solely to indicate this fact.

‖ To whom correspondence should be addressed: Dept. of Biochemistry and Molecular Biology, University of Florida, P. O. Box 100245, Gainesville, FL 32610-0245. Tel.: 352-392-8708; Fax: 352-392-6511; E-mail: lbloom@ufl.edu.

which binds δ with high affinity and physically blocks the region of δ that binds β (24, 26). When δ and δ′ are present in a complex with the γ subunits, the interaction between δ and δ′ is regulated by the γ subunits in an ATP-dependent manner (25). In the absence of ATP, the region of δ that binds β is buried within the complex, so the clamp loader is unable to open the clamp (24, 25). ATP binding to the γ subunits induces conformational changes (29) that expose this region of δ, allowing the clamp loader to bind with high affinity and to open the β clamp. ATP binding also increases the affinity of the clamp loader for DNA (30, 31), although a discrete DNA-binding site has not yet been identified. Subsequent binding to a primed template DNA triggers ATP hydrolysis, reducing the affinity of the clamp loader for β and DNA (31, 32). This reduced affinity is likely to be produced by conformational changes that mask β- and DNA-binding domains. Dissociation of the ADP-bound clamp loader from β and DNA allows the clamp to close and gives the polymerase access to the newly loaded clamp.

The precise nature of the ATP-induced conformational changes within the clamp loader is not yet known. Successive binding of ATP to each of the three γ subunits could potentially promote a series of conformational changes that ultimately produce an activated complex. Structural data for a minimal *E. coli* clamp loading complex ($\gamma_3\delta\delta'$) suggest that conformational changes that occur in each γ subunit are translated to the δ subunit, pulling it away from δ′ and exposing the β-binding domain (24). All 3 molecules of ATP are hydrolyzed when the γ complex releases the clamp on DNA (32, 33), but it is not yet known whether hydrolysis at specific sites is coupled to reducing interactions with DNA, whereas hydrolysis at other sites is coupled to releasing β. In this study, ATP hydrolysis and clamp loading reactions were measured under pre-steady-state conditions to define ATP-dependent steps. A key experiment was to measure the kinetics of ATP-dependent conformational changes by incubating the γ complex with ATP for different periods of time (0–1000 ms) to differentially populate conformational states that are formed upon binding ATP. DNA was then added to trigger ATP hydrolysis and to probe the relative populations of species present.

EXPERIMENTAL PROCEDURES

Nucleotides and Oligonucleotides—Concentrations of ATP (Amersham Biosciences) and ATPγS[1] (Roche Applied Science) solutions were determined by measuring the absorbance at 259 nm. Synthetic oligonucleotides were made on an ABI 392 DNA/RNA synthesizer using standard β-cyanoethyl phosphoramidite chemistry and reagents from Glen Research Corp. (Sterling, VA). Oligonucleotides were purified by denaturing PAGE. The sequences of the 105-nucleotide template and the complementary 30-nucleotide primer are as follows: 105-nucleotide template, 5′-GAG CGT CAA AAT GTA GGT ATT TCC ATG AGC GTT TTT CCt GTT GCA ATG GCT GGC GGT AAT ATT GTT CTG GAT ATT ACC AGC AAG GCC GAT AGT TTG AGT TCT TCT-3′; and 30-nucleotide primer, 5′-GAG CGT CAA AAT GTA GGT ATT TCC ATG AGC GTT TTT CCT GTT GCA ATG GC-3′. For anisotropy experiments, an amino linker (5′-Amino Modifier C6, Glen Research Corp.) was added to the 5′-end of the 105-mer and was covalently labeled with X-rhodamine isothiocyanate (Molecular Probes, Inc.) as described previously (30). Primed templates were annealed by incubating the 30-nucleotide primer with the 105-nucleotide template at 80 °C for 5 min and then allowing the solution to cool slowly to room temperature. For ATPase assays, the mole ratios of primer to template were 1.15:1 in annealing reactions and 1.2:1 in anisotropy assays. These primed templates were used without further purification (31).

DNA Polymerase III Proteins—DNA polymerase III proteins were purified, and the γ complex was reconstituted as described (2, 5). Proteins were stored in 20 mM Tris-HCl (pH 7.5), 2 mM dithiothreitol, 0.5 mM EDTA, and 10% glycerol. Assay buffer used for all experiments contained 20 mM Tris-HCl (pH 7.5), 50 mM NaCl, 8 mM $MgCl_2$, 5 mM dithiothreitol, and 40 μg/ml bovine serum albumin. The concentration of β was determined from its absorbance at 280 nm and the extinction coefficient (17, 900 M^{-1} cm^{-1}) for the native protein (34).

Concentrations of γ complex were determined from the absorbance at 280 nm in 6 M guanidine hydrochloride and the calculated extinction coefficient. This concentration was verified by amino acid analysis following acid hydrolysis of the protein (performed by the Protein Chemistry Core Facility, Biotechnology Program, University of Florida). A sample for amino acid analysis was prepared by dialyzing the γ complex against 20 mM sodium phosphate (pH 7.5) at 4 °C to remove glycerol and other buffer components that interfere with the analysis. The concentration of this dialyzed protein was also determined by three other methods for comparison: 1) its absorbance at 280 nm in 6 M guanidine hydrochloride (pH 6.5), 2) its concentration in a Bradford-type assay (Bio-Rad protein assay) using a bovine serum albumin standard, and 3) its concentration in a Bradford-type assay (Bio-Rad protein assay) using an IgG standard. The amino acid analysis and absorbance measured under denaturing conditions yielded concentrations of 1.6 μM and 1.7 μM, respectively (the same within experimental error). Both Bradford-type assays overestimated the concentration of protein by factors of 1.2 and 3.0 using the bovine serum albumin and IgG standards, respectively.

E. coli Phosphate-binding Protein (PBP)—PBP was purified and labeled with *N*-(2-(1-maleimidyl)ethyl)-7-(diethylamino)coumarin-3-carboxamide (MDCC; Molecular Probes, Inc.) by the method described by Brune *et al.* (35, 36), except that the "enhanced mop" was not used. MDCC-PBP was stored in 10 mM Tris-HCl (pH 8.0). The active-site concentration of MDCC-PBP was determined by titration with potassium phosphate standards. In each preparation, the concentration of active PBP correlated with the fraction of PBP that was labeled. This concentration of active MDCC-PBP was used in all calculations of P_i concentrations in ATPase assays.

Pre-steady-state ATPase Assays—ATP hydrolysis by the γ complex was measured using MDCC-PBP to report on P_i produced from the reaction. The increase in the fluorescence of MDCC-PBP upon binding P_i was measured in real time during the course of reactions as described (31, 33). Assay buffers contained a phosphate mop consisting of 0.14 units/ml purine-nucleotide phosphorylase (Sigma) and 168 μM 7-methylguanosine (Sigma) to remove P_i contamination from buffer components. Control reactions that contained no ATP were used to determine the intensity of MDCC-PBP in the absence of P_i (I_f), and reactions with 200 μM potassium phosphate gave a signal for completely bound MDCC-PBP (I_b) under a given set of experimental conditions. The fraction of MDCC-PBP bound to P_i at any time (t) during a hydrolysis reaction ($x_b(t)$) was calculated using the following equation: $x_b(t) = (I_{obs}(t) - I_f)/(I_b - I_f)$, where $I_{obs}(t)$ is the observed intensity at time t. The fraction bound was converted to the concentration bound by multiplying by the concentration of active MDCC-PBP. The concentration of P_i bound to MDCC-PBP is plotted as a function of time in Figs. 1, 4, and 5 to illustrate the number of molecules of ATP hydrolyzed per molecule of γ complex.

Assays were done using an Applied Photophysics SXMV stopped-flow apparatus and either single or sequential mixing protocols at 20 °C. Data were collected for a total of 12 s at intervals of 1 ms for the first 2 s and 5 ms thereafter. In single mixing experiments, the γ complex, MDCC-PBP, and DNA were placed in one syringe, and ATP was placed in a second. Reactions were initiated by mixing equal volumes from the two syringes. In sequential mixing experiments, the γ complex and β, when present, were placed in one syringe; ATP was placed in the second; and the third contained DNA and MDCC-PBP. The contents of the first two syringes were incubated in an aging loop for 15, 48, 98, 250, 500, or 1000 ms prior to adding the contents of the third syringe. Concentrations for each experiment are indicated under "Results."

ATPγS Chase Assays—Chase assays were performed as described for ATPase assays using the sequential mixing protocol with an incubation time of 1000 ms. In these assays, ATPγS was included in the third syringe along with DNA and MDCC-PBP. Final concentrations are given under "Results."

Pre-steady-state Fluorescence Anisotropy Experiments—Stopped-flow fluorescence anisotropy assays were done using a Biologic SFM-4 stopped-flow apparatus (Molecular Kinetics, Pullman, WA) equipped with four independently driven reagent syringes and a 30-μl cuvette (Model FC-15) with a 1.5-mm path length as described (31). For each experiment, vertically (I_{VV}) and horizontally (I_{VH}) polarized emission

[1] The abbreviations used are: ATPγS, adenosine 5′-*O*-(thiotriphosphate); PBP, *E. coli* phosphate-binding protein (*phoS* gene product); MDCC, *N*-(2-(1-maleimidyl)ethyl)-7-(diethylamino)coumarin-3-carboxamide; MDCC-PBP, PBP covalently labeled at Cys-197 with MDCC; RhX, X-rhodamine isothiocyanate; DNA-RhX, DNA substrate covalently labeled with RhX.

intensities were measured at 1-ms intervals for 8 s, and 19–20 stopped-flow runs were signal averaged. Anisotropy (r) was calculated from polarized intensities using Equation 1,

$$r = (I_{VV} - gI_{VH})/(I_{VV} + 2gI_{VH}) \quad \text{(Eq. 1)}$$

where g is the g-factor calculated by dividing the vertically polarized emission by the horizontally polarized emission measured when samples are excited with horizontally polarized light. Total intensities (I_{tot}) were also calculated for each reaction (Equation 2).

$$I_{tot} = I_{VV} + 2gI_{VH} \quad \text{(Eq. 2)}$$

There were no changes in the total intensities of X-rhodamine isothiocyanate (RhX) as a function of time, indicating that there were no changes in effective quantum yields during the course of the experiment. Therefore, anisotropy changes can be interpreted simply in terms of changes in rotational motion (37, 38). Three different mixing schemes were used to initiate clamp loading reactions as described under "Results"; but in each case, reagents from two syringes at 20 °C were mixed in equal volumes (80 μl) immediately before entering the cuvette.

Kinetic Modeling—The kinetic data in Fig. 4 were fit to the model shown in Fig. 5*A* using the program DynaFit (39). The code for this program was updated so that experiments in which two reagents are preincubated for a specified period of time prior to initiating reactions can be simulated and fit. To our knowledge, this is the only software available to model this type of kinetic assay. For these fits, the DNA binding rate was measured previously (31, 32), and the rate constant for binding was held constant at 300 μM^{-1} s^{-1} based on this work. The concentration of MDCC-PBP·P_i as a function of time was calculated by including experimentally determined rate constants for MDCC-PBP binding of P_i (35) as constants in the model. The total concentration of γ complex was treated as an adjustable parameter to account for the difference between total and active protein concentrations as well as the experimental accuracy of concentration and volume measurements. The fit yielded a concentration of 0.25 μM (93% active) γ complex for assays containing an experimentally determined concentration of 0.27 μM γ complex. Reaction time courses calculated from the model shown in Fig. 5*A* are plotted in Figs. 4 and 5*B*.

RESULTS

Pre-steady-state Kinetics of DNA-dependent ATP Hydrolysis by the γ Complex—ATP hydrolysis by the γ complex was measured in assays with and without the β clamp to determine how β alters the pre-steady-state reaction kinetics. A real-time fluorescence-based assay containing MDCC-PBP was used to measure the amount of P_i produced upon hydrolysis of ATP (33, 35). MDCC-PBP binds P_i in a 1:1 stoichiometry, and P_i binding produces an increase in the fluorescence of MDCC. Sequential mixing assays were performed by incubating the γ complex (0.27 μM) with ATP (100 μM) in the presence or absence of β (1 μM) for 1 s prior to adding a solution of DNA (1 μM) and MDCC-PBP (2.7 μM) to give the final concentrations indicated in parentheses. The concentration of P_i bound to MDCC-PBP (Fig. 1) was calculated from the increase in MDCC fluorescence to directly illustrate the number of ATP molecules hydrolyzed per molecule of γ complex in these experiments. The DNA substrate used in all experiments consisted of a 30-nucleotide primer annealed to a 105-nucleotide template, which supports loading of the β clamp and processive synthesis by the DNA polymerase III core (30, 31, 40).

In assays with the γ complex alone (Fig. 1*A*, *black trace*), the pre-steady-state kinetic data were biphasic, where the first phase was complete within ~100 ms, and the second phase took an additional 600 ms. The amplitudes of the rapid and slow phases were nearly equal, and their sum indicates that ~2.7 molecules of ATP were hydrolyzed per molecule of γ complex. Addition of β produced a single pre-steady-state phase of ATP hydrolysis that occurred at the more rapid rate (Fig. 1*B*, *inset*). The amplitude of this single phase indicates that 2.7 molecules of ATP/molecule of γ complex were also hydrolyzed in the presence of β. As reported previously (21), addition of β increases the steady-state rate of ATP hydrolysis.

Chase Experiments—ATPγS chase experiments were performed to determine the fate of ATP bound by the γ complex upon addition of DNA. These chase assays were done under sequential mixing conditions identical to those used for pre-steady-state ATPase assays, except that ATPγS (1 mM final concentration) was added to the solution of DNA and MDCC-PBP. ATPγS is hydrolyzed 4 orders of magnitude more slowly than ATP by the γ complex (41) and therefore is effectively non-hydrolyzable on the time scale of these experiments. In these assays, the γ complex is initially bound to ATP. Excess ATPγS will "trap" complexes that have lost ATP due to dissociation or that have hydrolyzed their bound ATP. If bound ATP is hydrolyzed more rapidly than it dissociates, then the first turnover of ATP should be unaffected. If ATP dissociation competes with hydrolysis, then the amount of ATP hydrolyzed in the first turnover will reflect relative rates of hydrolysis and dissociation. In ATPγS chase assays without β (Fig. 1*A*, *gray trace*), the rapid phase of ATP hydrolysis remained, but most of the ATP that was hydrolyzed in the slow phase was no longer hydrolyzed. In assays with β (Fig. 1*B*, *gray trace*), addition of ATPγS did not affect the amplitude of the burst of ATP hydrolysis, indicating that bound ATP is hydrolyzed more rapidly than it dissociates.

Together, these ATPase assays show that preincubation of the γ complex with ATP and β had a dramatic effect on the kinetics of hydrolysis. A key question is what gives rise to the biphasic kinetics of ATP hydrolysis in assays without β. The observation that the amplitudes of the two phases in assays without β were nearly equal suggests that two populations of the γ complex may be present: one that reacts more rapidly than the other.

Kinetics of ATP Hydrolysis when the γ Complex Is Not Equilibrated with ATP—ATP binding produces conformational changes in the clamp loader that increases its affinity for β and DNA (25, 26, 30, 31). To determine whether these conformational changes could contribute to the rate of hydrolysis, single mixing ATPase assays were done in which the γ complex was added directly to a solution of ATP, DNA, and MDCC-PBP. Reactions contained 0.27 μM γ complex, 1 μM DNA, and 2.7 μM MDCC-PBP and were carried out at several ATP concentrations (20, 80, 200, 400, and 800 μM). The increase in MDCC fluorescence arising from MDCC-PBP binding of P_i produced by hydrolysis was measured during the course of these reactions and is shown in Fig. 2. When the γ complex was not pre-equilibrated with ATP, a substantial lag preceded a rapid increase in fluorescence resulting from a burst of ATP hydrolysis. The length of the lag phase decreased with increasing concentrations of ATP and ranged from ~30 ms for ATP concentrations >200 μM to ~70 ms for 20 μM ATP. At ATP concentrations >200 μM, the length of the lag phase and the rate of increase in fluorescence were independent of ATP concentration. At these higher concentrations, the rate of ATP binding did not limit the observed rate of hydrolysis. Slow DNA binding is also unlikely to be responsible, as the reaction was faster when the γ complex was preincubated with ATP (Fig. 1*A*). Thus, an intramolecular reaction such as ATP-induced conformational changes in the γ complex is likely to limit the rate of hydrolysis under these conditions.

Effect of Equilibration of the γ Complex with ATP on the Kinetics of Clamp Loading—Pre-steady-state rates of ATP hydrolysis were faster when the γ complex was preincubated with ATP (Fig. 1) than when added directly to ATP and DNA (Fig. 2). To determine whether the rate of clamp loading was also dependent on preincubation of the γ complex with ATP, pre-steady-state clamp loading reactions were measured using a real-time fluorescence anisotropy-based assay. In this assay,

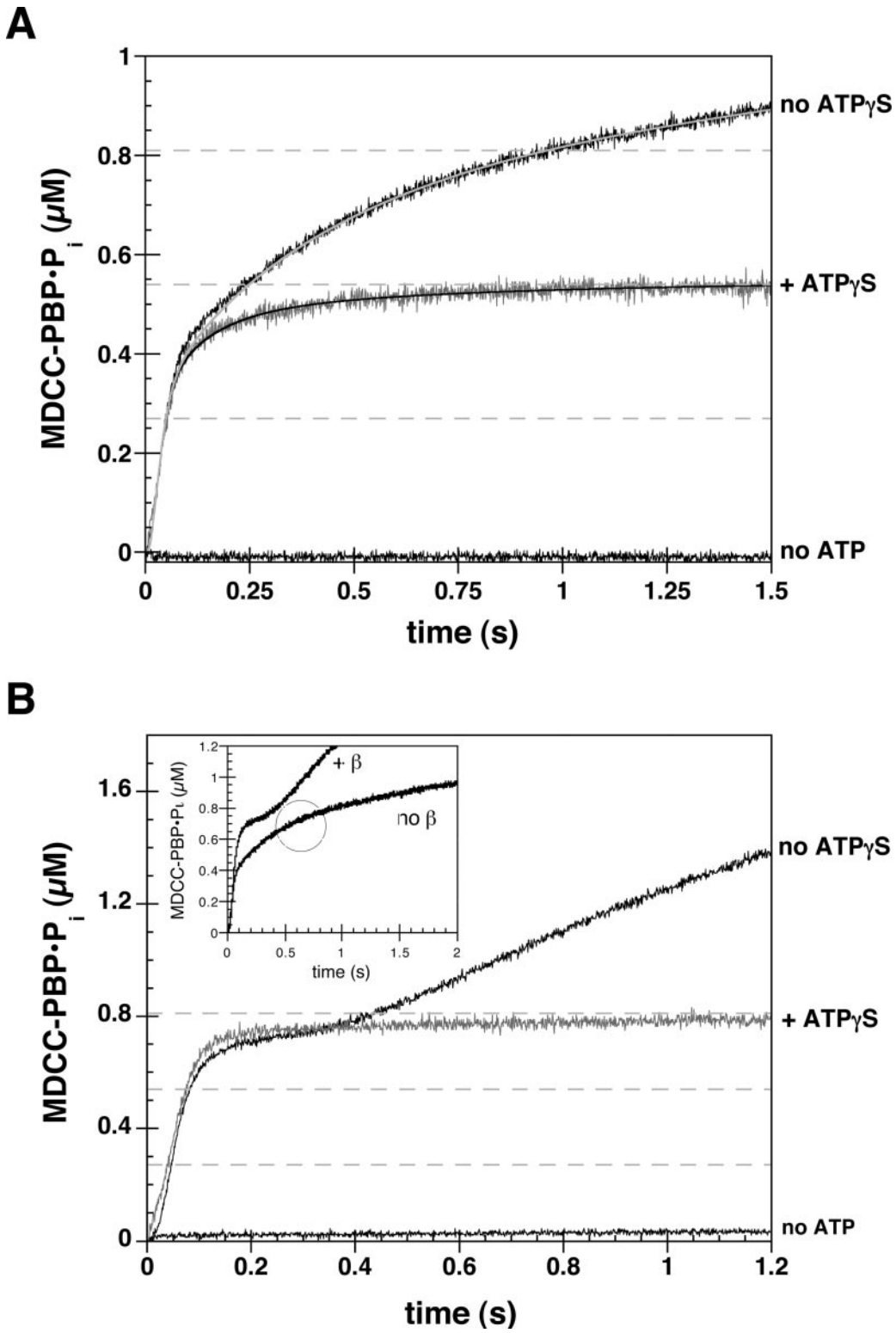

FIG. 1. **Pre-steady-state kinetics of ATP hydrolysis by the γ complex in the presence and absence of an ATPγS chase.** Sequential mixing experiments were performed in which the γ complex was incubated with ATP in the absence (*A*, *black trace*, *no ATPγS*) or presence (*B*, *black trace*, *no ATPγS*) of β for 1 s prior to addition of a solution containing DNA and MDCC-PBP. ATPγS chase experiments were done under identical conditions, except that ATPγS was included in a solution of DNA and MDCC-PBP (*gray traces*, + *ATPγS*). The increase in the fluorescence of MDCC when MDCC-PBP bound the P_i product of ATP hydrolysis was measured in real time. The concentration of MDCC-PBP bound to P_i was calculated from the increase in MDCC fluorescence and is plotted. Control experiments done in the absence of ATP (*black traces*, *no ATP*) showed no change. *Dashed gray lines* at MDCC-PBP•P_i concentrations of 0.27, 0.54, and 0.81 μM represent the amount of P_i formed from hydrolysis of 1, 2, and 3 molecules of ATP/molecule of γ complex, respectively. For direct comparison of burst amplitudes and rates in the presence and absence of β, data for reactions without the ATPγS chase are shown in the *inset* to *B*, where the transition from the pre-steady-state to the steady-state regimes is *circled* for the reaction with the γ complex alone. The *solid curves* through the data in *A* were calculated from the model in Fig. 5*A*, where ATPγS trapped the γ complex in the GC_1TTT and GC_3TDD states. The final reaction concentrations were 0.27 μM γ complex, 100 μM ATP, 1.0 μM β clamp (when present), 1.0 μM DNA, and 2.7 μM MDCC-PBP in assay buffer containing 20 mM Tris-HCl (pH 7.5), 50 mM NaCl, 8 mM $MgCl_2$, 5 mM dithiothreitol, and 40 μg/ml bovine serum albumin. In the ATPγS chase assays, ATPγS (1 mM final concentration) was added to the solution of DNA and MDCC-PBP.

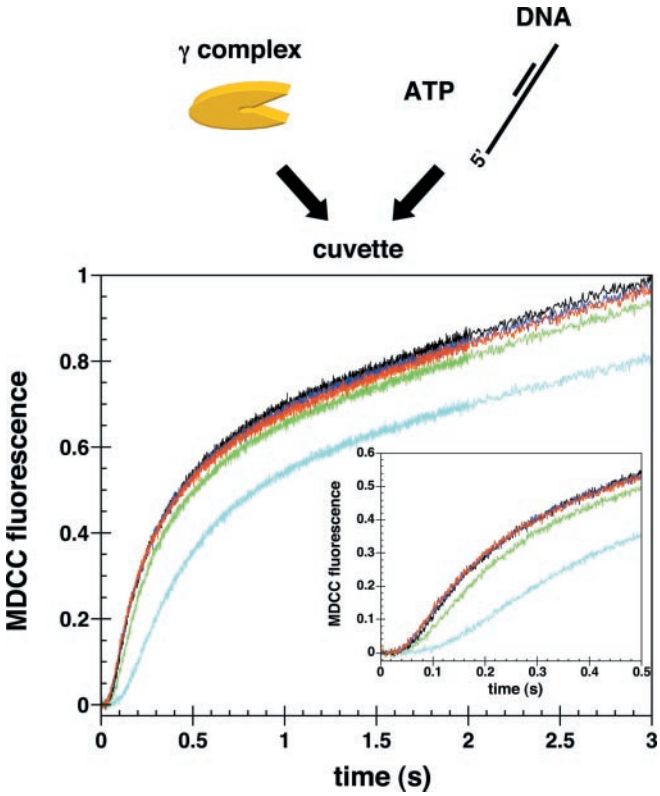

FIG. 2. **Kinetics of ATP hydrolysis in reactions initiated by addition of the γ complex to ATP and DNA.** Single mixing experiments were performed in which the γ complex (0.27 μM) was added directly to a solution of ATP (concentration varied), DNA (1.0 μM), and MDCC-PBP (2.7 μM) to give the concentrations indicated in assay buffer. Reactions contained 20 (*cyan*), 80 (*green*), 200 (*black*), 400 (*blue*), or 800 (*red*) μM ATP. ATP hydrolysis was measured by measuring the increase in the fluorescence of MDCC-PBP upon binding P_i, which is plotted as a function of time (in arbitrary units). The time base changes from 1- to 5-ms intervals at 2 s. The *inset* shows the first 0.5 s on an expanded scale.

the DNA substrate is covalently labeled with RhX (DNA-RhX), and the fluorescence anisotropy of RhX increases when DNA-RhX is bound by protein (30, 42). Polarized intensities of the RhX probe are measured during the time course of loading reactions and used to calculate the anisotropy of the probe as a function of time (38). Three different single mixing schemes were used to initiate clamp loading reactions. The same primed template DNA substrate was used in these assays as in ATPase assays, except that the template was labeled on the 5′-end with RhX. All reactions contained final concentrations of 0.25 μM γ complex, 500 μM ATP, 0.6 μM β, and 0.05 μM DNA-RhX.

In the first mixing scheme analogous to the ATPase assay in Fig. 1*B*, a solution of the γ complex, ATP, and β was added to an equal volume of a solution of DNA-RhX and ATP. Preincubation of the γ complex with ATP and β in these assays produced a rapid increase in anisotropy to a value of ~0.33 in the first 50–100 ms (Fig. 3*A*, *black trace*), followed by a slow decrease over ~500 ms to a steady-state value of ~0.3. The increase is most likely due to a β·γ complex binding to DNA, and the decrease due to dissociation of the γ complex from the clamp that has been loaded onto DNA (31, 43). The anisotropy (0.3) remains higher than free DNA (0.21) because a steady-state loading reaction is established (30).

In a second mixing scheme analogous to the ATPase assays in Fig. 2, the γ complex was added directly to a solution of ATP, β, and DNA-RhX. When reactions were initiated prior to ATP binding, a substantial lag of ~30 ms preceded an increase in anisotropy (Fig. 3*B*), as in ATPase assays (Fig. 2). This anisotropy increase (to a value of ~0.31) was complete in ~200 ms and was slow relative to the rate of the increase in Fig. 1*A*. The observed rate did not increase when the concentration of β was increased to 2.4 μM (Fig. 3*B*, *gray trace*); and thus, slow clamp loading is not the result of slow β binding. Slow DNA binding is also unlikely because the rate of DNA binding/clamp loading increased when the γ complex was preincubated with ATP and β. At ATP concentrations >100 μM, kinetic data for clamp loading were independent of ATP concentration (data not shown), indicating that ATP binding does not limit the observed rate of clamp loading. These results are consistent with those of the ATPase assays in Fig. 2 and indicate that an intramolecular reaction such as a conformational change limits the rate of the clamp loading reaction when the γ complex is not equilibrated with ATP.

In a third mixing scheme, a solution of the γ complex and ATP was added to a solution of β and DNA. When the γ complex was preincubated with ATP but not β, a biphasic increase in anisotropy was observed (Fig. 3*C*), reminiscent of the biphasic kinetics of ATP hydrolysis (Fig. 1*A*). The increase in anisotropy reached a maximal value of ~0.31 in 200 ms and was followed by a small decrease to a steady-state value of ~0.3. These biphasic kinetics indicate that two different species are present that bind DNA and/or load clamps at different rates.[2] This reaction time course resembles that for a mixture of reactions in which the γ complex was preincubated with ATP and β (Fig. 3*A*) and not incubated with ATP or β (Fig. 3*B*) and can be simulated empirically by a weighted sum of these time courses (Fig. 3*D*).[3]

The results from these clamp loading assays are consistent with those from ATP hydrolysis assays and indicate that a slow intramolecular reaction, most likely ATP-induced conformational changes in the γ complex, produces slow kinetics of clamp loading when the γ complex is not preincubated with ATP. After this slow reaction takes place, subsequent DNA binding is rapid (Fig. 3*A*).

Kinetics of ATP-induced Conformational Changes in the γ Complex—A series of sequential mixing reactions was performed in which the length of time that the γ complex was incubated with ATP was varied to measure the kinetics of ATP-induced conformational changes in the γ complex. If an ATP-induced conformational change limits the observed pre-steady-state rates of clamp loading and ATP hydrolysis in assays in which the γ complex is not preincubated with ATP, then the populations of conformational states should vary as a function of the incubation time with ATP. In these experiments, the γ complex was incubated with ATP for 0, 15, 48, 98, 250, 500, or 1000 ms prior to addition of DNA and MDCC-PBP (Fig. 4), and final concentrations were 0.27 μM γ complex, 400

[2] To test the possibility that these two species were free γ complex and a β·γ complex, this assay was repeated at two additional concentrations of β: 1.2 and 2.4 μM. There were no obvious differences in the kinetics with increasing concentrations of β (data not shown), suggesting that the two species are not free γ complex and a β·γ complex. Given the excess of β over DNA (12-, 24-, or 48-fold), it seems likely that the γ complex would bind β preferentially and that the two phases are the result of two different species of the γ complex that react at different rates. However, the signal-to-noise level in these assays may not be great enough to detect small differences, so we cannot conclusively rule out the possibility that the rapid phase is due to γ complex binding of DNA and the slow phase is due to γ complex binding of β prior to DNA.

[3] We have previously observed that the amplitude of the increase in anisotropy is related to the concentration of clamp loader under these conditions (30, 31). Based on this observation, we predict that if two species of the γ complex that reacted at different rates were present, the amplitudes of the phases due to the reaction of those species would be proportional to their concentrations. The concentrations of these species (GC_1TTT and GC_2TTT) were calculated from the rate constants in Fig. 5*A*.

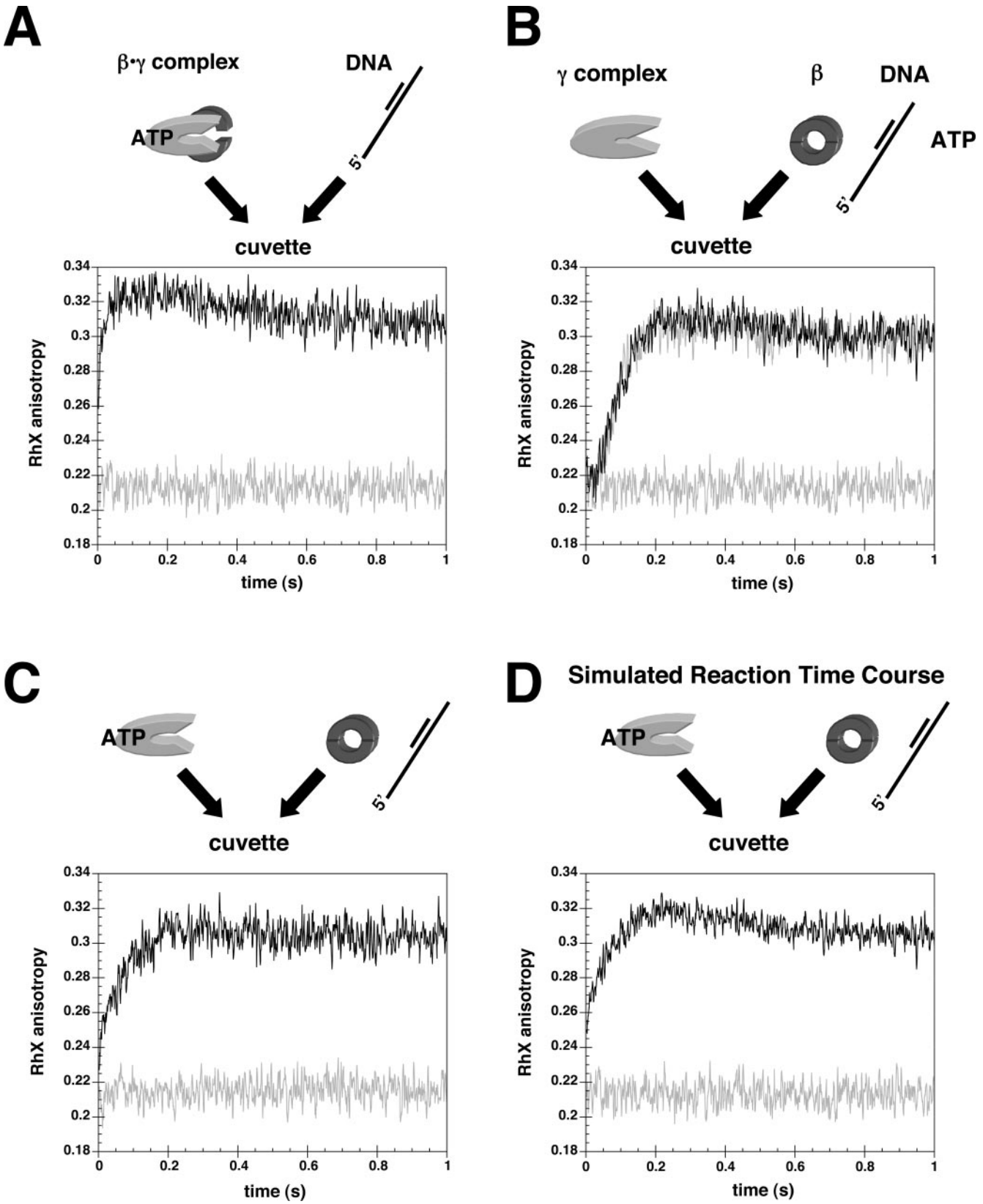

FIG. 3. **Kinetics of clamp loading measured in reactions initiated at different stages of the loading cycle.** The increase in anisotropy of an RhX probe covalently bound to DNA is plotted as a function of time for clamp loading reactions. The anisotropy of free DNA (*dark gray*) is also plotted and remains constant. *A*, reactions were initiated by addition of a solution of the γ complex, ATP, and β to a solution of DNA (*black trace*). *B*, reactions were initiated by addition of the γ complex to a solution of ATP, β, and the γ complex. The *black* and *gray traces* contained 0.6 and 2.4 μM β, respectively. *C*, reactions were initiated by addition of a solution of the γ complex and ATP to a solution of β and DNA. *D*, a reaction time course was empirically generated from a weighted sum of the data in *A* (62%) and *B* (38%). These percentages were chosen based on the model in Fig. 5*A*, where the relative equilibrium populations of GC_1TTT and GC_2TTT are 38 and 62%, respectively. Assays contained final concentrations of 0.25 μM γ complex, 0.6 μM β, 500 μM ATP, and 0.05 μM DNA in assay buffer.

μM ATP, 2.7 μM MDCC-PBP, and 1 μM DNA. The concentration of P_i produced by hydrolysis and bound to MDCC-PBP was calculated from the increase in the fluorescence of MDCC and is shown in Fig. 4. These data show the evolution of the rapid kinetics of hydrolysis produced when the γ complex was completely equilibrated with ATP. Shorter preincubation times showed a more pronounced lag and slower overall pre-steady-state rates of hydrolysis. Incubation of the γ complex with ATP for 250 ms or longer gave similar rates of hydrolysis, indicating that the conformational transitions have reached equilibrium by this point in time.

Kinetic Modeling of ATP Hydrolysis Reactions—Data from ATPase experiments in which the preincubation time with ATP was varied (Fig. 4) were modeled to define a minimal kinetic mechanism for the reaction. Because these data do not measure the DNA binding and release steps directly, rate constants for these steps were set based on previous analyses of DNA binding kinetics (31, 32). All other rate constants were obtained from global fitting (reviewed in Ref. 44) of data in Fig. 4 to the model shown in Fig. 5*A* using DynaFit (39). Some steps are described by a single forward observed rate constant because the data did not contain sufficient information to derive a unique pair of forward and reverse rate constants. This does not imply that these steps are chemically irreversible.

The model starts with ATP (T)-bound forms of the enzyme because the rate of hydrolysis was independent of ATP concentration (Fig. 2) under these assay conditions. The GC_1TTT state forms first and converts relatively slowly (k_{12} = 6.48 s^{-1}) to the GC_2TTT state. Increasing the incubation period with ATP increases the population of the GC_2TTT state and the observed pre-steady-state rate of ATP hydrolysis until an equilibrium is reached, where 62% of the γ complex exists in this state. DNA binding is a two-step reaction in which the initial binding of the GC_2TTT complex to DNA (N) is rapid and followed by a second step that generates a complex (GC_3TTTN) competent for hydrolysis. This two-step binding reaction is required to generate the slight lag in ATP hydrolysis while accommodating the rapid rate of DNA binding measured in anisotropy experiments (31, 32). It is possible that these two steps represent initial binding to the substrate, followed by a specific interaction with the primer-template junction that activates the complex for hydrolysis (32).

Kinetic data for ATPase assays performed with short preincubation times or without preincubation with ATP could not be fit to a model in which all 3 molecules of ATP were hydrolyzed at the same rate. The 3 molecules of ATP must be hydrolyzed at two different rates to obtain an adequate fit of these data to this model. Two molecules of ATP are hydrolyzed rapidly (k_{hydN} = 76 s^{-1}) in succession, and DNA is released upon hydrolysis of the 2nd molecule of ATP. A relatively slow change in this complex (k_{34} = 5.9 s^{-1}) must occur prior to slow hydrolysis (k_{hydB} = 2.9 s^{-1}) of the 3rd molecule of ATP. Previous studies have shown that DNA is released rapidly following hydrolysis of ATP (32, 33). For the model in Fig. 5 to fit both the previous DNA binding data and the kinetics of ATP hydrolysis measured in this study, DNA must be released following rapid hydrolysis of the 2nd molecule of ATP. Hydrolysis of the 3 ATP molecules at two different rates and the formation of two conformational states (GC_1TTT and GC_2TTT) upon equilibration with ATP produce biphasic kinetics of hydrolysis with roughly equal amplitudes.

In ATPase (Fig. 2) and clamp loading (Fig. 3*B*) assays in which the γ complex was not preincubated with ATP, a pronounced lag (~30 ms) in product formation was observed. The minimal model in Fig. 5 does not generate a lag that is long enough, but does fit these data if an additional species of the γ complex (GC_0TTT) that rapidly forms the first γ complex state (GC_1TTT) is included.[4] The data shown in Fig. 5*B* from an ATPase assay in which the γ complex was not preincubated with ATP were fit to the model in Fig. 5*A* by inclusion of this additional step and by making the last step

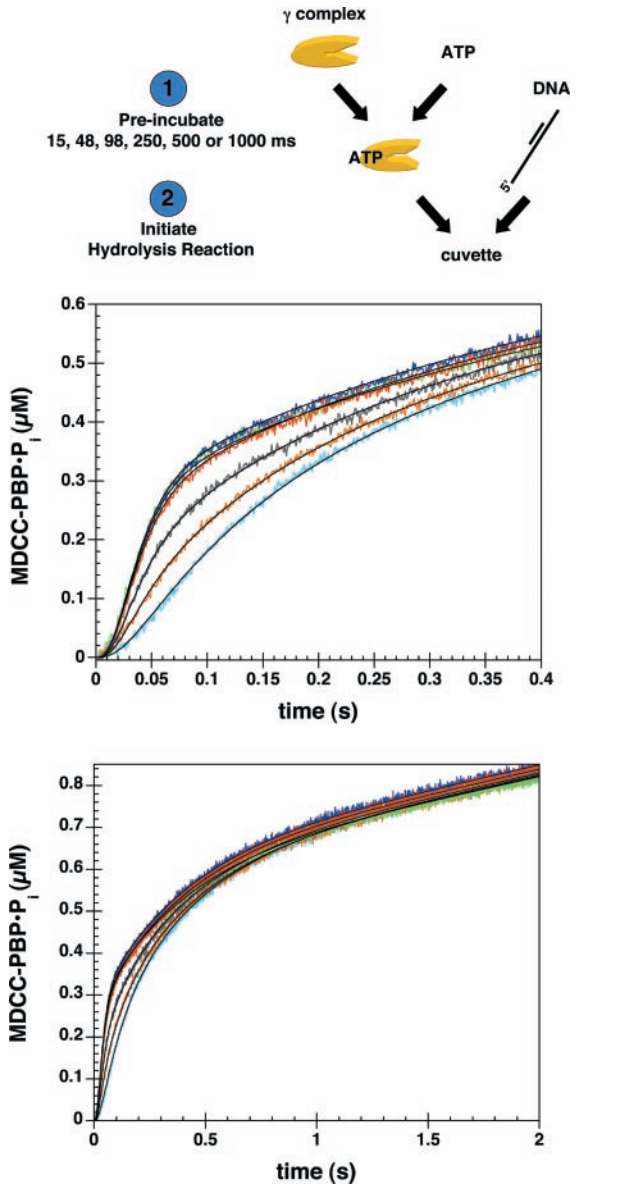

FIG. 4. **Kinetics of ATP hydrolysis upon incubation of the γ complex with ATP for a defined period of time prior to addition of DNA.** Sequential mixing experiments were performed in which the γ complex was incubated with ATP for 15 (*cyan*), 48 (*orange*), 98 (*gray*), 250 (*red*), 500 (*blue*), or 1000 (*green*) ms prior to addition of DNA and MDCC-PBP. The increase in the fluorescence of MDCC-PBP upon binding P_i was measured as a function of time and used to calculate the concentration of P_i produced by hydrolysis and bound to MDCC-PBP. The concentration of MDCC-PBP·P_i is plotted as a function of time on time scales of 0.4 s (*upper panel*) and 2 s (*lower panel*). Data were collected at 1-ms intervals for the first 2 s and at 5-ms intervals from 2 to 12 s (not shown). The *solid black curves* through the data were calculated by fitting the data to the model shown in Fig. 5*A*. The final concentrations were 0.27 μM γ complex, 400 μM ATP, 1.0 μM DNA, and 2.7 μM MDCC-PBP in assay buffer.

[4] The data in Fig. 4 can also be fit by inclusion of this additional step ($GC_0TTT \rightarrow GC_1TTT$); however, this step is not well defined by these data because it is rapid relative to the shortest preincubation period with ATP that is experimentally accessible. The half-life of this reaction is 11 ms, whereas the shortest preincubation time is 15 ms.

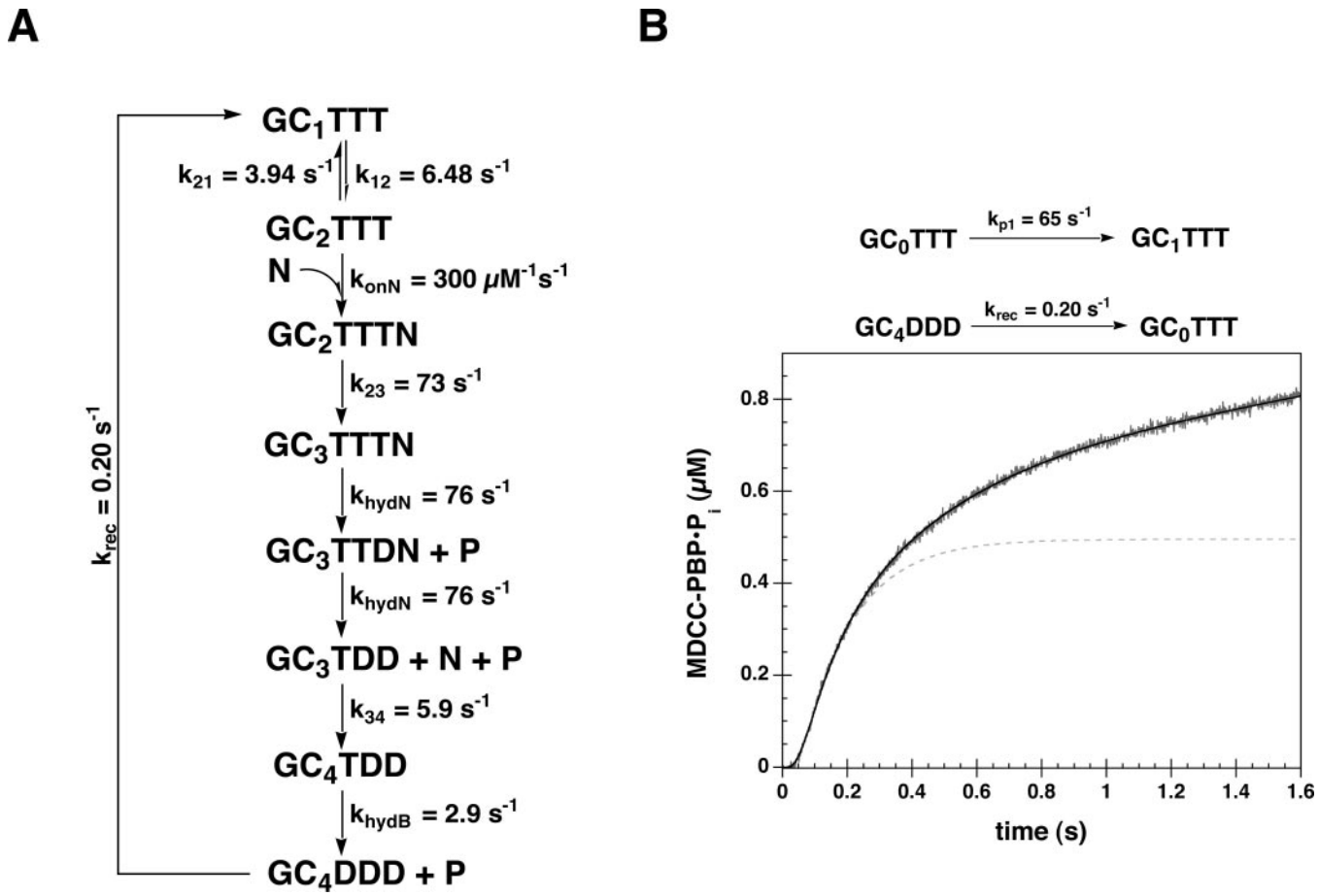

FIG. 5. **Kinetic modeling of ATP hydrolysis reactions.** *A*, the kinetic model and rate constants used to fit data in Fig. 4 are shown. This model has two key features. First, addition of ATP (T) to the γ complex (GC) initially forms a GC_1TTT state, which converts to a new species (GC_2TTT) relatively slowly. Both of these species are present when the γ complex is equilibrated with ATP (preincubation times ≥250 ms). The GC_2TTT complex is activated for binding DNA and subsequent ATP hydrolysis. A second feature of this model is that 2 of the 3 molecules of ATP are hydrolyzed rapidly, forming ADP (D) and P_i (P) with DNA release upon hydrolysis of the 2nd molecule. The 3rd molecule is hydrolyzed slowly after the complex is no longer bound to DNA. In fitting the data, the DNA binding rate constant (k_{onN} = 300 $\mu M^{-1}s^{-1}$) (31, 32) and the rate constants for P_i binding to MDCC-PBP (k_{onP} = 136 μM^{-1} s^{-1}) (35) and dissociating from MDCC-PBP (k_{offP} = 13.6 s^{-1}) (35) were set to values that were measured directly in other work. All other rate constants were derived from fitting the data in Fig. 4 to the model shown using DynaFit (39). The steady-state portions of the reactions are described by a pseudo first-order reaction that "recycles" the final ADP-bound state to the initial ATP-bound state. This pseudo first-order approximation is reasonable because only a very small fraction of the ATP substrate (<0.2%) is consumed on the time scale of the reaction. *B*, the kinetic model shown in *A* requires an additional step to generate the lag in ATP hydrolysis in reactions in which the γ complex is not preincubated with ATP. A single mixing assay was performed in which the γ complex (0.27 μM) was added to ATP (500 μM), DNA (1.0 μM), and MDCC-PBP (2.7 μM) to give the final concentrations indicated in assay buffer. The *solid black curve* through the data was calculated from the model and rate constants in *A* with the inclusion of the two steps shown above the graph. A rapid step (k_{p1} = 65 s^{-1}) that initially forms the GC_1TTT state was added, and the final recycling step in *A* was changed so that the GC_4DDD state regenerated the GC_0TTT state rather than the GC_1TTT state. The rate constants k_{p1} and k_{rec} were fit as adjustable parameters, but all other rate constants were set to the values shown in *A*. The first turnover of ATP is biphasic under these assay conditions, although the two phases are difficult to identify by visual inspection alone. The *dashed gray line* through the data shows the calculated time course for hydrolysis of the first 2 molecules of ATP, which occurs at a more rapid rate than hydrolysis of the remaining ATP molecule.

recycle to the GC_0TTT state rather than to the GC_1TTT state. The calculated curve was generated using the rate constants shown in Fig. 5*A* and fitting only k_{p1} and k_{rec} as adjustable parameters. Although the observed rate of this reaction is independent of ATP concentration under these conditions, ATP binding will require some finite time and may be reflected in this additional step.

DISCUSSION

The *E. coli* γ complex functions as a molecular machine to assemble ring-shaped β clamps on primers where DNA synthesis is slated to begin (reviewed in Ref. 45). This mechanical task requires that the affinity of the clamp loader for β and DNA be modulated during the course of the clamp loading cycle. Initially, the γ complex must have a high affinity for both β and DNA to efficiently bring them together. ATP binding produces a high affinity binding state (25, 26, 31) in which the δ subunit can bind the clamp and "crack" it open (26–28). Thus, ATP binding allows the γ complex to form a ternary clamp loader·clamp·DNA complex (43) in which an open clamp is most likely encircling DNA. At this point, the affinity of the clamp loader for the clamp and DNA must be reduced so that the clamp can be closed around DNA and the γ complex can dissociate so as not to interfere with the polymerase binding the newly loaded clamp. A primed template DNA provides the trigger to convert the γ complex to a low affinity binding state (31, 32). Upon binding a primer end, the γ complex hydrolyzes ATP and releases the clamp and DNA (32).

Binding and hydrolysis of ATP most likely induce conformational changes that produce the high and low affinity binding states, respectively (24, 25, 31). Each clamp loader can hydrolyze up to 3 molecules of ATP, as each γ subunit has an ATP-binding site. These binding sites are located at the inter-

face of two domains within a γ subunit and also at the interface between two adjacent subunits within the complex (24, 29). ATP binding by each γ subunit is likely to promote a conformational change within that subunit, which is then communicated to adjacent subunits. Thus, multiple conformational changes within the complex are likely to be associated with the transition to a high affinity binding state. Ultimately, this combination of conformational changes exposes a region on the N-terminal domain of the δ subunit that binds the clamp. The conformational changes also expose or create a DNA-binding domain that has not yet been identified. Although it has been demonstrated that all 3 molecules of ATP are hydrolyzed upon release of the clamp on DNA (33), it is not yet known whether one subset of γ subunits hydrolyzes ATP to break the interaction with the clamp, whereas another subset hydrolyzes ATP to release DNA. This work addresses this question by measuring ATP hydrolysis and clamp loading under pre-steady-state conditions to gain a greater insight into the ATP-dependent steps in the clamp loading reaction.

When the γ complex was equilibrated with ATP (preincubation times ≥250 ms), the first turnover of ATP occurred in two phases of nearly equal amplitude, and the sum of the amplitudes indicated that 2.7 molecules of ATP were hydrolyzed per molecule of γ complex (Fig. 1*A*). In assays with the clamp, a single phase of hydrolysis occurred at the same rate as the rapid phase in assays without β, and the same number of ATP molecules was hydrolyzed, ~1 molecule/binding site (Fig. 1*B*). Together, these data suggest that two populations of the γ complex may be present in the absence of β, each of which hydrolyzes 3 molecules of ATP, and that β converts the two to a single species. The most obvious physical explanation is that the two species of the γ complex represent two conformational states related by relatively slow ATP-induced changes; one population has undergone conformational changes that activate it for DNA binding/clamp loading, and the other has not. If this were the case, then in ATPase (Fig. 2) and clamp loading (Fig. 3*B*) assays in which the γ complex was not preincubated with ATP, the entire population of clamp loader must start from the state that has not undergone the conformational changes. The prediction would then be that the rates of the pre-steady-state phases of ATP hydrolysis and clamp loading in these assays would be slower, as was observed experimentally. A forward rate constant for the conformational change step of ~6.5 s^{-1} for reactions at 20 °C was calculated from the model presented in Fig. 5*A*. Although it is relatively slow, this calculated rate constant is rapid enough to be consistent with rates of clamp loading that are required for DNA synthesis on the lagging strand where a clamp must be loaded for synthesis of each Okazaki fragment. The half-life of this reaction is on the order of 110 ms, and the reaction could easily be achieved in the 2 s that it takes the polymerase to synthesize a 2-kb Okazaki fragment.

Why would the γ complex exist in two conformational states in the presence of ATP? One possibility is that both of these states need to be accessible for clamp loading, and this is achieved by making them nearly energetically equivalent. The activated state not only may be in the optimal conformation for high affinity binding to the clamp and DNA, but may also form a "tight" complex in which ATP dissociation is relatively slow. The other conformation may represent a "loose" state that allows nucleotide exchange and recharging of the clamp loader with ATP. Results from ATPγS chase experiments (Fig. 1) are consistent with this possibility. All the ATP hydrolyzed in the rapid phase by the activated complex was hydrolyzed in the presence of ATPγS, whereas most of the ATP hydrolyzed in the slow phase was exchanged for ATPγS. If β does selectively bind the activated conformation and shift the equilibrium toward this state, then *in vivo*, where the concentration of β is relatively high, the loose state would not be significantly populated and would exist only transiently during the nucleotide reloading process.

To define the kinetics of the ATP-induced conformational changes, ATP hydrolysis by the γ complex in the absence of β was measured in assays in which the γ complex was preincubated with ATP for a defined time to differentially populate the two major conformational states before adding DNA to trigger hydrolysis (Fig. 4). Kinetic modeling of these assays together with the "no preincubation" experiment (Figs. 2 and 5*B*) revealed that two phases of ATP hydrolysis persisted in these experiments. Because the rate of the rapid phase was reduced relative to experiments in which the γ complex was preincubated with ATP for times >250 ms, these two phases are difficult to identify by visual inspection alone. Any kinetic model that fits the ATP hydrolysis data must have two key features: 1) at least two populations of γ complex formed upon equilibration with ATP that are on the linear pathway to products and 2) a step that partitions ATP hydrolysis so that a fraction of ATP is hydrolyzed slowly. The model proposed in Fig. 5*A* achieves this by including two species of the γ complex (GC_1TTT and GC_2TTT) that are formed sequentially upon addition of ATP and by rapid hydrolysis of 2 molecules of ATP and slow hydrolysis of the 3rd molecule. Although we favor a model in which 1 of the ATP molecules is hydrolyzed slowly, it is formally possible that hydrolysis is rapid, but that release of the P_i product from hydrolysis of 1 molecule is slow. The fluorescence-based ATPase assay does not report on hydrolysis until P_i is released into solution. Therefore, a mechanism in which hydrolysis is rapid but P_i release is slow would also produce a slow increase in fluorescence. However, experiments done using radiolabeled ATP (40) that measure hydrolysis directly gave kinetic data that are in agreement with the kinetic data reported here, suggesting that the fluorescence-based assay gives an accurate measure of hydrolysis rates.

A key prediction of the model in Fig. 5*A* is that hydrolysis of 2 molecules of ATP is associated with conformational changes that reduce binding interactions with DNA, whereas hydrolysis of the 3rd molecule is associated with conformational changes that retract the δ subunit and release the clamp. If DNA were released upon hydrolysis of the 3rd molecule of ATP, the rate of dissociation would be too slow to be consistent with previous measurements of DNA binding and release rates (31–33). One way to reconcile the kinetics of ATP hydrolysis with the kinetics of DNA release is for DNA to be released following the rapid hydrolysis of the first 2 molecules of ATP. Previous work has shown that a primed template DNA specifically triggers hydrolysis of ATP (32). Perhaps binding interactions with primed templates are required to induce formation of a conformational state that gives rise to efficient hydrolysis of ATP at two of the binding sites. Hydrolysis of the 3rd molecule (or release of P_i from the third site) may be slow in assays without β because the β clamp may be required to generate the appropriate conformation for efficient hydrolysis at the third site. Thus, the β clamp may increase the overall rate of hydrolysis by affecting the kinetics of two steps: increasing the population of the activated GC_2TTT state by preferential binding to this state and stimulation of ATP hydrolysis at the third binding site by facilitating formation of the optimal conformation. Together, these two events would convert the biphasic kinetics of ATP hydrolysis in the absence of the clamp to a single pre-steady-state phase of ATP hydrolysis (Fig. 1).

In summary, this work suggests a model for clamp loading in which two conformational states of the clamp loader exist in

the presence of ATP: one that is activated for DNA and β binding and one that is not. The activated complex is formed from the other in a relatively slow reaction that most likely represents ATP-induced conformational changes in the γ complex. The γ complex hydrolyzes 3 molecules of ATP upon releasing the clamp on DNA, but hydrolysis at two sites may be coupled to changes that reduce the affinity of the clamp loader for DNA, whereas hydrolysis at the third site may release the clamp. Distinct roles for ATP at individual sites are supported by the results in the accompanying article (46). Experiments with site-directed mutants of the γ complex suggest that ATP binding at two sites is coupled to formation of a high affinity DNA binding state and that ATP binding at the third site is coupled to formation of a high affinity clamp binding state.

REFERENCES

1. Fay, P. J., Johanson, K. O., McHenry, C. S., and Bambara, R. A. (1981) *J. Biol. Chem.* **256,** 976–983
2. Kong, X.-P., Onrust, R., O'Donnell, M., and Kuriyan, J. (1992) *Cell* **69,** 425–437
3. Gulbis, J. M., Kelman, Z., Hurwitz, J., O'Donnell, M., and Kuriyan, J. (1996) *Cell* **87,** 297–306
4. Maki, S., and Kornberg, K. (1988) *J. Biol. Chem.* **263,** 6555–6560
5. Onrust, R., Finkelstein, J., Naktinis, V., Turner, J., Fang, L., and O'Donnell, M. (1995) *J. Biol. Chem.* **270,** 13348–13357
6. Pritchard, A. E., Dallman, H. G., Glover, B. P., and McHenry, C. S. (2000) *EMBO J.* **19,** 6536–6545
7. Blinkowa, A. L., and Walker, J. R. (1990) *Nucleic Acids Res.* **18,** 1725–1729
8. Tsuchihashi, Z., and Kornberg, A. (1990) *Proc. Natl. Acad. Sci. U. S. A.* **87,** 2516–2520
9. Flower, A. M., and McHenry, C. S. (1990) *Proc. Natl. Acad. Sci. U. S. A.* **87,** 3713–3717
10. McHenry, C. S. (1982) *J. Biol. Chem.* **257,** 2657–2663
11. Hawker, J. R., Jr., and McHenry, C. S. (1987) *J. Biol. Chem.* **262,** 12722–12727
12. Maki, H., Maki, S., and Kornberg, A. (1988) *J. Biol. Chem.* **263,** 6570–6578
13. Studwell-Vaughan, P. S., and O'Donnell, M. (1991) *J. Biol. Chem.* **266,** 19833–19841
14. Onrust, R., Finkelstein, J., Turner, J., Naktinis, V., and O'Donnell, M. (1995) *J. Biol. Chem.* **270,** 13366–13377
15. Kim, S., Dallman, H. G., McHenry, C. S., and Marians, K. J. (1996) *Cell* **84,** 643–650
16. Yuzhakov, A., Turner, J., and O'Donnell, M. (1996) *Cell* **86,** 877–886
17. Gao, D., and McHenry, C. S. (2001) *J. Biol. Chem.* **276,** 4441–4446
18. Wu, C. A., Zechner, E. L., Hughes, A. J., Jr., Franden, M. A., McHenry, C. S., and Marians, K. J. (1992) *J. Biol. Chem.* **267,** 4064–4073
19. Leu, F. P., Georgescu, R., and O'Donnell, M. (2003) *Mol. Cell* **11,** 315–327
20. Dallmann, H. G., Thimmig, R. L., and McHenry, C. S. (1995) *J. Biol. Chem.* **270,** 29555–29562
21. Onrust, R., Stukenberg, P. T., and O'Donnell, M. (1991) *J. Biol. Chem.* **266,** 21681–21686
22. Onrust, R., and O'Donnell, M. (1993) *J. Biol. Chem.* **268,** 11766–11772
23. Olson, M. W., Dallmann, H. G., and McHenry, C. S. (1995) *J. Biol. Chem.* **270,** 29570–29577
24. Jeruzalmi, D., O'Donnell, M., and Kuriyan, J. (2001) *Cell* **106,** 429–441
25. Naktinis, V., Onrust, R., Fang, F., and O'Donnell, M. (1995) *J. Biol. Chem.* **270,** 13358–13365
26. Turner, J., Hingorani, M. M., Kelman, Z., and O'Donnell, M. (1999) *EMBO J.* **18,** 771–783
27. Stewart, J., Hingorani, M. M., Kelman, Z., and O'Donnell, M. (2001) *J. Biol. Chem.* **276,** 19182–19189
28. Leu, F. P., Hingorani, M. M., Turner, J., and O'Donnell, M. (2000) *J. Biol. Chem.* **275,** 34609–34618
29. Podobnik, M., Weitze, T. F., O'Donnell, M., and Kuriyan, J. (2003) *Structure* **11,** 253–263
30. Bloom, L. B., Turner, J., Kelman, Z., Beechem, J. M., O'Donnell, M., and Goodman, M. F. (1996) *J. Biol. Chem.* **271,** 30699–30708
31. Ason, B., Bertram, J. G., Hingorani, M. M., Beechem, J. M., O'Donnell, M., Goodman, M. F., and Bloom, L. B. (2000) *J. Biol. Chem.* **275,** 3006–3015
32. Ason, B., Handayani, R., Williams, C. R., Bertram, J. G., Hingorani, M. M., O'Donnell, M., Goodman, M. F., and Bloom, L. B. (2003) *J. Biol. Chem.* **278,** 10033–10040
33. Bertram, J. G., Bloom, L. B., Hingorani, M. M., Beechem, J. M., O'Donnell, M., and Goodman, M. F. (2000) *J. Biol. Chem.* **275,** 28413–28420
34. Johanson, K. O., Haynes, T. E., and McHenry, C. S. (1986) *J. Biol. Chem.* **261,** 11460–11465
35. Brune, M., Hunter, J. L., Corrie, J. E. T., and Webb, M. R. (1994) *Biochemistry* **33,** 8262–8271
36. Brune, M., Hunter, J. L., Howell, S. A., Martin, S. R., Hazlett, T. L., Corrie, J. E., and Webb, M. R. (1998) *Biochemistry* **37,** 10370–10380
37. Otto, M. R., Lillo, M. P., and Beechem, J. M. (1994) *Biophys. J.* **67,** 2511–2521
38. Lakowicz, J. R. (1999) *Principles of Fluorescence Spectroscopy*, pp. 291–320, Plenum Publishing Corp., New York
39. Kuzmič, P. (1996) *Anal. Biochem.* **237,** 260–273
40. Hingorani, M. M., Bloom, L. B., Goodman, M. F., and O'Donnell, M. (1999) *EMBO J.* **18,** 5131–5144
41. Hingorani, M. M., and O'Donnell, M. (1998) *J. Biol. Chem.* **273,** 24550–24563
42. Perez-Howard, G. M., Weil, P. A., and Beechem, J. M. (1995) *Biochemistry* **34,** 8005–8017
43. Bertram, J. G., Bloom, L. B., Turner, J., O'Donnell, M., Beechem, J. M., and Goodman, M. F. (1998) *J. Biol. Chem.* **273,** 24564–24574
44. Beechem, J. M. (1992) *Methods Enzymol.* **210,** 37–54
45. Davey, M. J., Jeruzalmi, D., Kuriyan, J., and O'Donnell, M. (2002) *Nat. Rev. Mol. Cell Biol.* **3,** 826–835
46. Snyder, A. K., Williams, C. R., Johnson, A., O'Donnell, M., and Bloom, L. B. (2004) *J. Biol. Chem.* **279,** 4386–4393